THE JOURNAL OF BIOLOGICAL CHEMISTRY
Vol. 275, No. 49, Issue of December 8, pp. 38445–38451, 2000

Printed in U.S.A.

Niemann-Pick Type C1 (NPC1) Overexpression Alters Cellular Cholesterol Homeostasis*

Received for publication, April 13, 2000, and in revised form, August 7, 2000
Published, JBC Papers in Press, August 29, 2000, DOI 10.1074/jbc.M003180200

Elizabeth E. Millard‡, Kalpana Srivastava‡, Linton M. Traub§, Jean E. Schaffer‡¶, and Daniel S. Ory‡‖

From the ‡Center for Cardiovascular Research, Department of Internal Medicine and the ¶Department of Molecular Biology and Pharmacology, Washington University School of Medicine, St. Louis, Missouri 63110-1010, and the §Department of Cell Biology and Physiology, University of Pittsburgh School of Medicine, Pittsburgh, PA 15261

The Niemann-Pick type C1 (NPC1) protein is a key participant in intracellular trafficking of low density lipoprotein cholesterol, but its role in regulation of sterol homeostasis is not well understood. To characterize further the function of NPC1, we generated stable Chinese hamster ovary (CHO) cell lines overexpressing the human NPC1 protein (CHO/NPC1). NPC1 overexpression increases the rate of trafficking of low density lipoprotein cholesterol to the endoplasmic reticulum and the rate of delivery of endosomal cholesterol to the plasma membrane (PM). CHO/NPC1 cells exhibit a 1.5-fold increase in total cellular cholesterol and up to a 2.9-fold increase in PM cholesterol. This increase in PM cholesterol is closely paralleled by a 3-fold increase in *de novo* cholesterol synthesis. Inhibition of cholesterol synthesis results in marked redistribution of PM cholesterol to intracellular sites, suggesting an unsuspected role for NPC1 in internalization of PM cholesterol. Despite elevated total cellular cholesterol, CHO/NPC1 cells exhibit increased cholesterol synthesis, which may be attributable to both resistance to oxysterol suppression of sterol-regulated gene expression and to reduced endoplasmic reticulum cholesterol levels under basal conditions. Taken together, these studies provide important new insights into the role of NPC1 in the determination of the levels and distribution of cellular cholesterol.

Intracellular cholesterol sorting and transport pathways play an important role in the physiologic utilization of lipoprotein-derived cholesterol. Low density lipoprotein (LDL)[1] and modified lipoprotein particles are trafficked to lysosomes, where the cholesteryl esters are hydrolyzed to free cholesterol (1). The bulk of LDL cholesterol is mobilized from lysosomes to the plasma membrane (PM) and subsequently cycles back to the endoplasmic reticulum (ER) (2). Approximately one-third of the unesterified lysosomal cholesterol is delivered directly to the ER via a PM-independent transport pathway (3). Cholesterol levels in the ER regulate cellular cholesterol homeostasis through a feedback regulatory mechanism that controls *de novo* synthesis and cellular uptake of cholesterol. This regulatory system principally involves membrane-bound transcription factors known as sterol regulatory element-binding proteins (SREBPs) (4). When cells are sterol-depleted, the NH_2-terminal regions of the SREBPs are released through a two-step proteolytic cleavage and translocate to the nucleus to promote transcription of multiple genes involved in cholesterol and fatty acid homeostasis. When cells are replete with sterols, proteolytic cleavage of SREBPs is prevented, resulting in attenuation of SREBP-dependent gene transcription.

The Niemann-Pick type C1 (NPC1) protein has been identified as a key participant in the intracellular trafficking of LDL cholesterol. Cells that harbor mutations in NPC1 accumulate cholesterol in lysosomes and exhibit delayed sterol-regulated gene expression (5). The human *NPC1* gene and its murine ortholog have been identified by positional cloning methods (6, 7). The 1278-amino acid human NPC1 protein has 13 predicted membrane-spanning domains (8), five of which share sequence homology with the putative sterol-sensing domains of 3-hydroxy-3-methylglutaryl-coenzyme A reductase, SREBP cleavage-activating protein (SCAP), and Patched. In normal cells, NPC1 is located in a vesicular compartment, which is LAMP-2-positive and mannose-6-phosphate receptor-negative (9). When cells are treated with hydrophobic amines to block intracellular cholesterol trafficking, the NPC1 protein co-localizes with sequestered cholesterol in lysosomes (9).

Although previous studies show that NPC1 is required for mobilization of LDL cholesterol from endosomes to the PM (2, 10, 11) and for delivery of PM cholesterol to the ER for esterification (3, 11), the role of NPC1 in cholesterol homeostasis is not well understood. To further characterize the function of NPC1, we generated stable Chinese hamster ovary (CHO) cell lines that overexpress NPC1 and examined intracellular trafficking of LDL cholesterol and regulation of cellular sterol homeostasis. In these cell lines the NPC1 protein is expressed in physiologically appropriate cellular compartments, as demonstrated by immunofluorescence and by stimulation of cholesterol trafficking. Overexpression of NPC1 is associated with abnormal regulation of cellular cholesterol content and distribution. These results further our understanding of the relationship between cholesterol trafficking and cellular cholesterol homeostasis.

* This work was supported by grants from the National Niemann-Pick Disease Foundation (to D. S. O.) and the National Science Foundation (to E. E. M.). The costs of publication of this article were defrayed in part by the payment of page charges. This article must therefore be hereby marked "*advertisement*" in accordance with 18 U.S.C. Section 1734 solely to indicate this fact.

‖ To whom correspondence should be addressed: Center for Cardiovascular Research, Washington University School of Medicine, Box 8086, 660 S. Euclid Ave., St. Louis, MO 63110. Tel.: 314-362-8737; Fax: 314-362-0186; E-mail: dory@imgate.wustl.edu.

[1] The abbreviations used are: LDL, low density lipoprotein; CL-LDL, cholesteryl linoleate LDL; CD, β-hydroxypropylcyclodextrin; CHO, Chinese hamster ovary; ER, endoplasmic reticulum; 25-HC, 25-hydroxycholesterol; NPC1, Niemann-Pick type C1; PBS, phosphate-buffered saline; PM, plasma membrane; SRE, sterol regulatory element; SREBP, sterol regulatory element-binding protein; SCAP, SREBP cleavage-activating protein; SSD, sterol-sensing domain; U18666A, 3-β-(2-diethylaminoethoxy)androst-5-en-17-one; NSF, normal skin fibroblasts.

EXPERIMENTAL PROCEDURES

Materials—Dulbecco's modified Eagle's medium, Ham's F-12 medium, fetal calf serum, glutamine, penicillin/streptomycin, and LipofectAMINE Plus were obtained from Life Technologies, Inc. Lipoprotein-deficient fetal calf serum was obtained from Cocalico Labs. Cholesterol oxidase was obtained from Calbiochem. U18666A was obtained from Biomol. Compactin, β-hydroxypropylcyclodextrin (CD), filipin complex, human LDL, mevalonic acid, oleoyl-CoA, and sphingomyelinase were obtained from Sigma. LysoSensor Green DND-153 was obtained from Molecular Probes. Oleic acid, triolein, and cholesteryl oleate were obtained from Nu-Check Prep. Cholesterol, cholestenone, and 25-hydroxycholesterol (25-HC) were obtained from Steraloids. [^{3}H]Cholesterol (75 Ci/mmol), *N*-[9,10-^{3}H]oleic acid (5 Ci/mmol), *N*-[*cholesteryl*-1,2,6,7-^{3}H]linoleate (84 Ci/mmol), [*oleate*-1-^{14}C]cholesteryl oleate (59.5 mCi/mmol), [1-^{14}C]oleoyl-Co-A (50 mCi/mmol), and [1,2-^{14}C]acetic acid (54 mCi/mmol) were obtained from PerkinElmer Life Sciences.

Plasmids—The human NPC1 cDNA in pSPORT-NPC1 was provided by J. Strauss (University of Pennsylvania). A ΔU3hNPC1 construct was created by polymerase chain reaction using pSPORT-NPC1 as template and the following primers: 5′-GCTCTAGACTGCCATGACCGCTCGCGGCCTGGC-3′ and 5′-CGGGATCCCAGGATGCCCTGCGAGAGGGC-3′. The 3.8-kilobase polymerase chain reaction product was digested with *Xba*I and *Bam*HI and subcloned into the *Xba*I and *Bam*HI cloning sites of the ΔU3 retroviral construct (12). All polymerase chain reaction-derived sequences were confirmed by ABI Prism automated sequencing. The pSyn sterol regulatory element (SRE) plasmid was a gift of R. Deckelbaum and T. Osborne (13). The pCMVβgal used as a transfection control consists of the *lacZ* gene driven by a cytomegalovirus promoter.

Cell Lines—CHO-K1 cells were obtained from ATCC (CRL-9618). CT60 cells, a CHO cell line that harbors mutations in NPC1 and SCAP, were provided by T. Y. Chang (Dartmouth College). M12 cells are mutant CHO-K1 cells that contain a deletion of the NPC1 locus.[2] To generate the CHO/NPC1 cell lines, CHO-K1 cells were infected with retrovirus prepared by transient transfection of 293GPG-packaging cells with the ΔU3hNPC1 construct (12). The retrovirally infected cells were plated at limiting dilution, and colonies were screened by Western blot analysis of microsomal fractions for human NPC1 expression (described under "Western Blot Analysis").

Cell Culture and Preparation of Reconstituted LDL—Cells were maintained in monolayer culture at 37 °C with 5% CO_2. All CHO cell lines were maintained in medium A (1:1 Dulbecco's modified Eagle's medium:Ham's F-12, 5% (v/v) fetal calf serum, 2 mM glutamine, 50 units/ml penicillin, 50 μg/ml streptomycin). Medium B consists of medium A in which fetal calf serum has been replaced with 5% (v/v) lipoprotein-deficient fetal calf serum. Medium C consists of medium B plus 20 μM compactin and 0.5 mM mevalonate. Compactin and mevalonate were prepared as described (14). 293GPG cells were grown in Dulbecco's modified Eagle's medium with 10% (v/v) fetal calf serum, 2 mM glutamine, 50 units/ml penicillin, 50 μg/ml streptomycin, 2 μg/ml puromycin, 0.3 μg/ml G418, and 1 μg/ml tetracycline. LDL labeled with [^{3}H]cholesteryl linoleate (CL) ([^{3}H]CL-LDL) was prepared with a specific activity of 17,000 cpm/nmol of total cholesteryl linoleate (15).

Western Blot Analysis—Microsomal proteins were prepared as described previously (16) and non-boiled samples were resolved on SDS-polyacrylamide gel electrophoresis (7.5%) under reducing conditions. The gels were transferred onto nitrocellulose (0.45 mm; Schleicher & Schuell) with a semi-dry electroblotter (Owl Scientific). Western blot analysis of NPC1 expression was performed using a rabbit polyclonal antibody raised against human NPC1 (amino acids 1261–1278) at a dilution of 1:1000 and a peroxidase-conjugated F(ab′)$_2$ fragment donkey anti-rabbit IgG (Jackson ImmunoResearch Laboratories) at 0.04 μg/ml. Detection was performed using a commercially available reagent (Renaissance, DuPont NEN).

Immunocytochemical Staining of NPC1 and Filipin Staining—On day 0, CHO cell lines were plated at 0.7×10^4 cells/well on 12-mm glass coverslips in 24-well dishes in medium A. For cells treated with U18666A, media was replaced 8–10 h after plating with U18666A (2 μg/ml) in medium A. On day 1, the cells were washed twice with PBS and fixed with 4% paraformaldehyde in PBS for 30 min. For experiments with LysoSensor staining, cells were incubated with 5 μM LysoSensor Green DND-153 for 2 h before fixation and staining. The cells were washed twice with PBS and stained (and permeabilized) with 50 μg/ml filipin in PBS/10% normal goat serum for 30 min. The cells were then stained for NPC1 using an affinity-purified antibody to the human NPC1 COOH terminus (amino acids 1261–1278). The cells were incubated with a 1:250 dilution of the α-NPC1 antibody in filipin/PBS/10% normal goat serum for 60 min on a shaker at 37 °C followed by incubation with a donkey anti-rabbit Cy3 secondary antibody at 5 μg/ml filipin/PBS/10% normal goat serum for 40 min on a shaker at 37 °C. The coverslips were washed three times with PBS, mounted (SlowFade, Molecular Probes), and examined by fluorescence microscopy on a Zeiss Axiovert epifluorescence microscope. The following filter sets (Chroma) were used: for filipin, excitation filter 360/40 nm, beamsplitter 400 nm, emission filter 460/50 nm; for LysoSensor, excitation filter 470/40 nm, beamsplitter 500 nm, emission filter 535/40 nm; for Cy3, excitation filter 535/50 nm, beamsplitter 565 nm, emission filter 590 nm.

LDL-stimulated Cholesterol Esterification Assay—Cholesterol esterification assays were performed as described by Goldstein *et al.* (17). On day 0, CHO cell lines were seeded in triplicate (2.5×10^4 cells/35-mm well) in medium A. On day 1, the cells were washed twice with PBS and refed medium B. On day 2, the cells were fed medium B with 50 μg/ml LDL. On day 3, the cells were pulsed with [^{3}H]oleate for 2 h and washed three times with Tris-buffered saline at 4 °C, and lipids were extracted with hexane:isopropyl alcohol (3:2). A chromatography recovery standard was added (30 μg cholesteryl oleate, 30 μg triolein, 0.0005 μCi [^{14}C]cholesteryl oleate), and the samples were dried under nitrogen. The lipids were separated by TLC (PE SIL G plates, Whatman) using heptane:ethyl ether:acetic acid (90:30:1) and visualized with iodine. The [^{3}H]cholesteryl oleate was quantified by liquid scintillation counting in Ecoscint (National Diagnostics). After lipid extraction, monolayers were incubated with 0.1 N NaOH, and protein determination was performed using the MicroBCA assay (Pierce). LDL-specific cholesterol esterification was determined by subtracting esterification rates for non-LDL-fed cells from LDL-fed cells.

Cholesterol Efflux Assay—On day 0, CHO, M12, and CHO/NPC1 cells were seeded in triplicate (5×10^4 cells/35-mm well) in medium A. On day 2, the cells were washed three times with PBS and refed medium B. On day 3, the cells were fed 20 μg/ml of [^{3}H]CL-LDL in medium B plus 20 μg/ml progesterone. On day 4, the cells were washed three times with PBS and incubated with medium B plus 2% CD for up to 2 h. Lipids were extracted from the media (CH_3Cl:methanol (2:1)) and the cells (hexane:isopropyl alcohol (3:2)), a recovery standard was added (0.0005 μCi [^{14}C]cholesteryl oleate for media lipid samples; 80 μg cholesterol, 30 μg cholesteryl oleate, and 0.0005 μCi [^{14}C]cholesteryl oleate for cellular lipid samples), and lipids were dried under nitrogen. Lipids were extracted from media by CH_3Cl:methanol (2:1), and cellular lipids were separated by TLC as described above using heptane:isopropyl ether:acetic acid (60:40:4) as the solvent. [^{3}H]Cholesterol was quantified by scintillation counting. Protein determinations were performed using the MicroBCA assay. The percent cholesterol efflux was determined as the amount of [^{3}H]cholesterol in the medium divided by the sum of the [^{3}H]cholesterol in medium plus the [^{3}H]cholesterol in the cell extract.

Cholesterol Oxidase Treatment—Cholesterol oxidase treatment was performed as described previously (3). On day 0, CHO, M12, and CHO/NPC1 cell lines were seeded in triplicate (5×10^4 cells/35-mm well) in medium A. On day 2, the cells were washed twice with PBS and refed medium B. On day 3, the cells were fed either medium B or medium C with 1 μCi [^{3}H]cholesterol/well. On day 4, each well was washed three times with Tris-buffered saline plus 2 mg/ml bovine serum albumin (Sigma) at 4 °C for 5 min on a shaker, and rapidly washed twice with PBS at room temperature. The cells were fixed in 1% glutaraldehyde in PBS for 10 min at room temperature and incubated with cholesterol oxidase (2 units/well) and sphingomyelinase (0.1 units/well) in Ham's F-12 for 30 min at 37 °C. The cells were washed twice with PBS, and lipids were extracted as described above. A chromatography recovery standard was added (20 μg cholesterol, 40 μg cholestenone, 30 μg cholesteryl oleate, 0.0005 μCi [^{14}C]cholesteryl oleate), and the samples were dried under nitrogen. TLC was performed as above using heptane:ethyl ether:acetic acid (90:30:1) as the solvent. [^{3}H]Cholesterol, [^{3}H]cholestenone, and [^{3}H]cholesteryl oleate were quantified as described above. Protein determinations were performed on parallel wells plated in triplicate using the MicroBCA assay.

Assay of de Novo Cholesterol Synthesis—Metabolic labeling of *de novo*-synthesized cholesterol was performed as described previously (18). On day 0, CHO, M12, CT60, and CHO/NPC1 cells were seeded in triplicate in (2.5×10^4 cells/35-mm well) in medium A. On day 1, the cells were washed three times with PBS and refed medium B. On day 2, the cells were washed three times with PBS and refed medium B with 0.5 mM [^{14}C]acetate (25 dpm/pmol). After a 2-h incubation, the cells were washed three times with Tris-buffered saline at 4 °C, and lipids were extracted as described above. A chromatography recovery stand-

[2] E. E. Millard, K. Srivastava, L. M. Traub, J. E. Schaffer, and D. S. Ory, unpublished results.

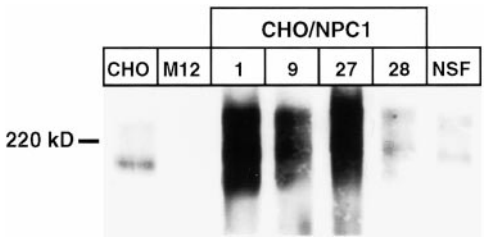

FIG. 1. **NPC1 overexpression in CHO cell lines.** CHO cell lines overexpressing human NPC1 were screened for NPC1 expression. Microsomal proteins (CHO and M12 cell lines, 80 μg; CHO/NPC1 cell lines and human NSF, 10 μg) were separated by SDS-polyacrylamide gel electrophoresis and analyzed by Western blotting using an antibody to the COOH terminus of NPC1, horseradish peroxidase-coupled secondary antibody, and chemiluminescence.

ard was added (20 μg cholesterol, 30 μg cholesteryl oleate, 0.002 μCi [^{3}H]cholesterol), and the samples were dried under a stream of nitrogen. TLC and [^{14}C]cholesterol quantification was performed as described under "Cholesterol Oxidase Treatment," and protein determination was performed using the MicroBCA assay.

Luciferase Reporter Assay—On day 0, CHO, CT60, and CHO/NPC1 cells were plated in duplicate (6×10^5 cells/60-mm dish) in medium A. On day 1, the cells were co-transfected with 1.5 μg of pSyn SRE and 0.5 μg of pCMVβgal. Four hours post-transfection, the media was changed to medium C supplemented with 0–1.0 μg/ml 25-HC. On day 2, cells were harvested in reporter lysis buffer (Promega), and luciferase and β-galactosidase assays were performed in duplicate for each sample. The luciferase activity in the transfected cells was normalized to β-galactosidase expression to correct for transfection efficiency.

In Vitro Cholesterol Esterification Assay—The *in vitro* esterification assay was performed as described by Lange and Steck (19). Cells were trypsinized, pelleted, and washed in 0.25 M sucrose, 5 mM sodium phosphate, pH 7.5. Pelleted cells were resuspended in 0.1 M sucrose, 5 mM sodium phosphate, pH 7.5, and swelled on ice for 10 min. The cells were homogenized with a Dounce homogenizer (100–200 strokes), centrifuged to remove large particles, and adjusted to 1 mM dithiothreitol and 1 mg/ml bovine serum albumin. The esterification reaction was started by the addition of 25 μM [^{14}C]oleoyl-CoA followed by incubation for 2 h at 37 °C. After extraction with CH_3Cl:methanol (2:1) and addition of a recovery standard (40 μg cholesterol, 30 μg cholesteryl oleate, 0.002 μCi [^{3}H]cholesterol), lipids were dried under nitrogen. Cholesteryl oleate was recovered by TLC and quantified as described under "LDL-stimulated Cholesterol Esterification Assay." Protein determinations were performed using the BCA assay.

RESULTS

Isolation of CHO Cell Lines Overexpressing NPC1—To study the function of NPC1, we used a retroviral expression system to establish stable CHO cell lines that overexpress NPC1. The human NPC1 cDNA was cloned into the ΔU3 retroviral vector and transfected into 293GPG-packaging cells to generate high titer virus encoding NPC1 (12). The virus was used to infect CHO cells at high multiplicity of infection, and clonal cell lines were isolated by plating at limiting dilution. The clones were screened for NPC1 expression by Western blotting of microsomal proteins with an antibody to the COOH terminus of NPC1 (amino acids 1261–1278) (Fig. 1). This antibody recognizes proteins of 220 and 170 kDa in wild-type CHO cells and detects no protein in M12 cells in which the NPC1 locus has been deleted.[2] We observe an identical pattern on Western blots using a previously characterized antibody to NPC1 residues 1256–1274 (data not shown) (20). The 220- and 170-kDa bands likely represent heterogeneously glycosylated NPC1 and have been observed by others (21). Because the COOH termini of human and hamster NPC1 only share 78% identity from residues 1261–1278, the NPC1 antibody demonstrates a preference for recognition of human over endogenous CHO sequences (note the 8-fold difference in amount of protein loaded in CHO *versus* CHO/NPC1 and human normal skin fibroblasts (*NSF*) *lanes*). Therefore, to estimate levels of transgene expression,

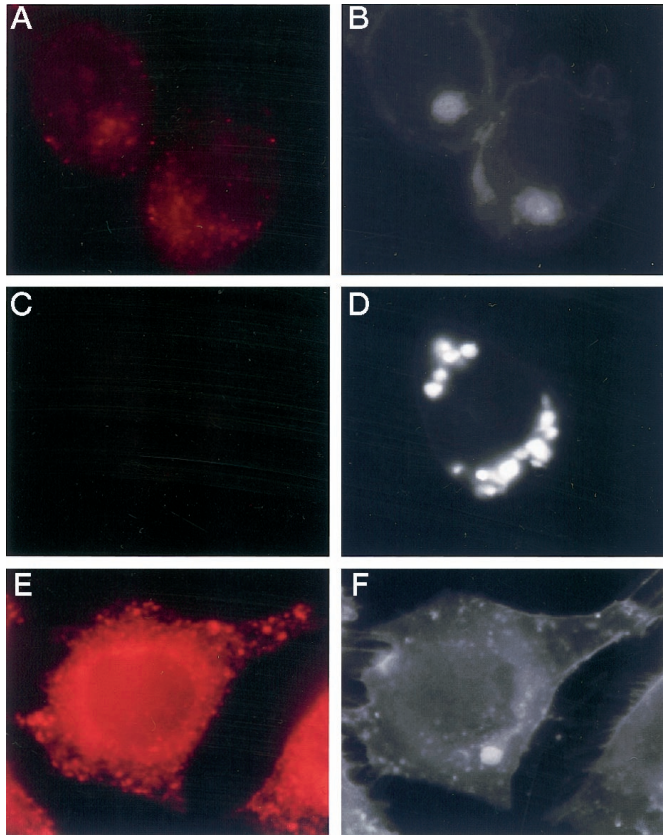

FIG. 2. **Distribution of NPC1 in NPC1-overexpressing CHO cells.** Wild-type CHO (*A* and *B*), M12 (*C* and *D*) and NPC1–1 cells (*E* and *F*) were plated in medium A and co-stained with an antibody to the COOH terminus of NPC1 (*A*, *C*, and *E*) and filipin 50 μg/ml (*B*, *D*, and *F*). Cells were examined by immunofluorescence microscopy.

we compared NPC1 expression in the CHO/NPC1 cell lines with the endogenous NPC1 expression in human NSF. Among the CHO/NPC1 cell lines, expression of NPC1 varies over a 12-fold range, with NPC1–1 ≈ NPC1–27 > NPC1–9 > NPC1–28. The lowest expressing CHO/NPC1 cell line, NPC1–28, expressed human NPC1 at a level 1.3-fold above NSF. The highest expressing CHO/NPC1 cell line, NPC1–1, expressed human NPC1 at a level 15-fold above NSF.

Immunofluorescence studies were performed to confirm the expression of NPC1 in these cell lines and to establish that when overexpressed in CHO cells, the human NPC1 protein distributes to appropriate cellular compartments. We co-stained fixed, permeabilized cells with affinity-purified antibody to the NPC1 COOH terminus and with filipin, a fluorescent polyene antibiotic that specifically binds unesterified cholesterol (22). In wild-type CHO cells under basal conditions (Fig. 2*A*), weak staining for NPC1 was observed in granular structures that have been identified in previous studies as late endosomes (9). This staining was not observed in controls with secondary antibody-staining alone (data not shown). Filipin staining was observed in a Golgi-like pattern and at the cell periphery (Fig. 2*B*). NPC1-staining was not observed in the NPC1-null, filipin-positive M12 cell line (Fig. 2, *C* and *D*). In CHO/NPC1 cell lines, robust NPC1 staining was observed in granular and reticular structures (Fig. 2*E*). Filipin primarily stained the PM and granular structures in the CHO/NPC1 cells (Fig. 2*F*). The intensity of filipin staining exceeded that of parental CHO cells, suggesting that these cells have increased cellular cholesterol content.

To show that overexpressed NPC1 is also appropriately localized in the setting of pharmacologic block of cholesterol

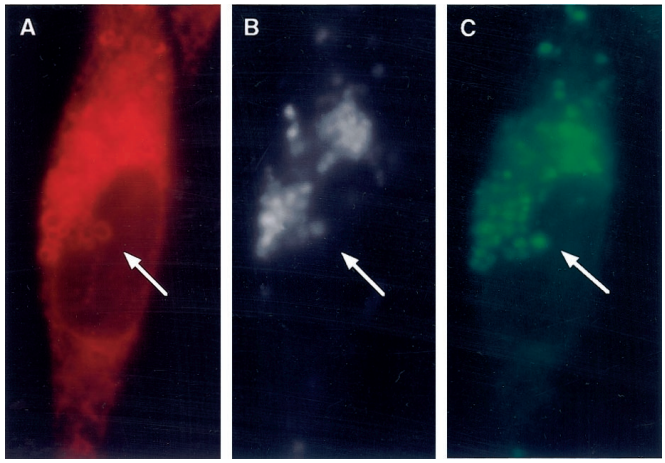

FIG. 3. **Distribution of NPC1 in U18666A-treated CHO/NPC1 cells.** On day 0, CHO/NPC1 cells were plated in medium A and incubated with 2 μg/ml U18666A. On day 1, cells were incubated with 5 μM LysoSensor Green DND-153 for 2 h before fixation and stained for NPC1 (*A*) and filipin (*B*). Acidic organelles were visualized using the LysoSensor probe (*C*). Cells were examined by immunofluorescence microscopy.

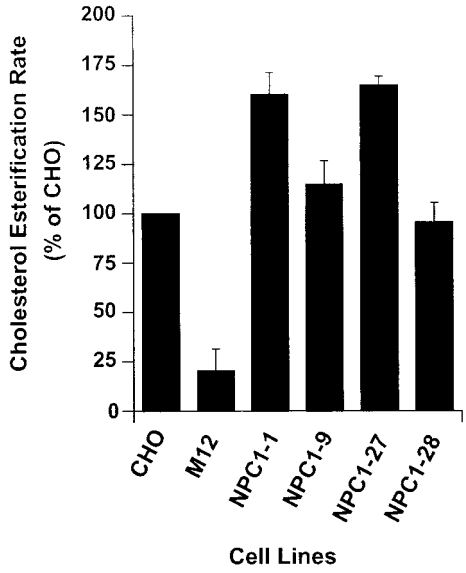

FIG. 4. **Increased LDL-stimulated cholesterol esterification in NPC1-overexpressing cell lines.** Cells were plated in triplicate in medium A (2.5×10^4 cells/35-mm well) and then grown in medium B for 48 h. The cells were fed LDL (50 μg/ml) for 16 h and then pulsed for 2 h with [^{3}H]oleate. The rate of incorporation of [^{3}H]oleate into cholesteryl [^{3}H]oleate was determined by scintillation counting after lipid extraction and TLC and normalized to total cellular protein. LDL-specific cholesterol esterification was determined by subtracting esterification rates for non-LDL-fed wells from LDL-fed wells. Esterification rates (pmol/min/mg) were normalized to wild-type CHO cells. Values are means ± S.E. and are representative two independent experiments.

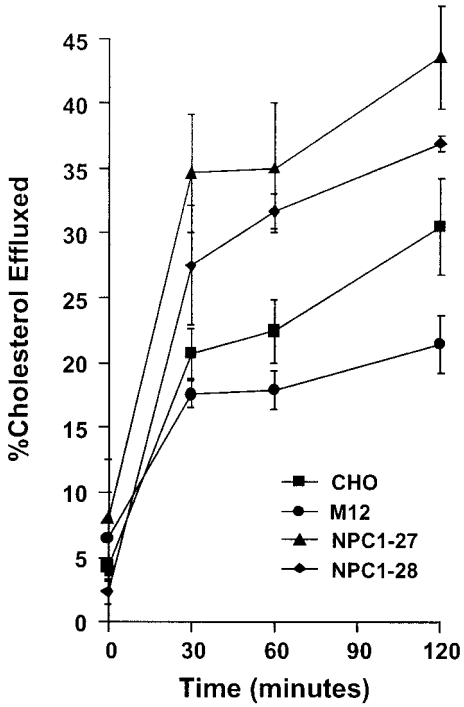

FIG. 5. **Increased delivery of cholesterol to the PM in CHO/NPC1 cells.** Cells were plated in triplicate in (5×10^4 cells/35-mm well) in medium A, then grown in medium B for 24 h. The cells were incubated for 24 h with 20 μg/ml of [^{3}H]CL-LDL in medium B plus 20 μg/ml progesterone. The following day the cells were washed with PBS and incubated with medium B plus 2% CD for up to 2 h. [^{3}H]Cholesterol was extracted from the media, and rates of cholesterol efflux were determined. Values are means ± S.E. and are representative of four independent experiments.

trafficking, CHO/NPC1 cells were incubated with U18666A. This hydrophobic amine inhibits mobilization of lysosomal cholesterol and results in the NPC mutant phenotype (10). U18666A-treated cells were co-stained with an antibody for NPC1, filipin, and a LysoSensor probe that specifically stains acidic organelles (23). After treatment with U18666A, there was a decrease in the granular NPC1-staining pattern and appearance of multiple, large, perinuclear vesicular structures whose periphery stains intensely for NPC1 (Fig. 3*A*, see *arrows*). Many of these structures are cholesterol-rich as demonstrated by filipin staining (Fig. 3*B*) and co-stain with LysoSensor probe (Fig. 3*C*), consistent with a late endosomal or lysosomal localization. This pattern of circumferential staining around cholesterol-containing vesicular structures after U18666A treatment is similar to the staining we have observed in mutant cell lines that have normal NPC1 expression but genetic blocks in the cholesterol-trafficking pathway.[3]

Overexpressed NPC1 Affects Cellular Cholesterol Trafficking—To characterize the effects of NPC1 overexpression on LDL cholesterol trafficking, we compared LDL-stimulated cholesterol esterification in wild-type CHO, M12, and CHO/NPC1 cell lines. In normal cells, uptake of LDL cholesterol expands the cellular cholesterol pool and activates acyl-CoA:cholesterol *O*-acyltransferase (ACAT), catalyzing the esterification of both *de novo*-synthesized and LDL-derived cholesterol in the ER (3). Cells were incubated in medium B, fed LDL 50 μg/ml overnight, and pulsed for 2 h with [^{3}H]oleate. Esterification rates, as determined by incorporation of [^{3}H]oleate into [^{3}H]cholesteryl oleate, are shown in Fig. 4 as a percentage of the rate observed for wild-type CHO cells. As expected, M12 cells have severely impaired LDL-stimulated cholesterol esterification rates (20% of wild-type CHO cells). Overexpression of NPC1 results in up to a 60% increase in esterification rates compared with wild-type CHO cells and up to an 8.1-fold increase compared with M12 cells. The observed esterification rates correlated with the level of NPC1 expression by Western blotting, suggesting a dose-dependent relationship between the amount of NPC1 protein and the delivery of LDL cholesterol to acyl-CoA:cholesterol *O*-acyltransferase.

We also examined the effect of NPC1 overexpression on the delivery of endosomal cholesterol to the PM. CHO and CHO/

[3] A. Frolov, K. Srivastava, D. Daphna-Iken, L. M. Traub, J. E. Schaffer, and D. S. Ory, manuscript in preparation.

NPC1 cells were incubated with progesterone and [^{3}H]CL-LDL for 24 h and treated with 2% CD for up to 2 h, and the rates of cholesterol efflux were measured during a progesterone washout phase. After a 2-h incubation with CD, cholesterol efflux from the M12 cells was decreased by 30% as compared with wild-type CHO cells (Fig. 5). NPC1 overexpression increased cholesterol efflux in the NPC1–27 and NPC1–28 cell lines by 43 and 21%, respectively, as compared with wild-type CHO cells. These findings are consistent with previous studies that support a role for NPC1 in the mobilization of lysosomal cholesterol (2, 10, 11). Taken together, the immunofluorescence, cholesterol esterification, and cholesterol efflux studies provide evidence that the exogenously expressed NPC1 in our stable cell lines is targeted to appropriate cellular membranes and functions in the trafficking of LDL cholesterol in a biologically relevant manner.

NPC1 Overexpression Affects Cholesterol Homeostasis—We anticipated that increased trafficking of LDL cholesterol to the ER and PM in the CHO/NPC1 cells might alter the partitioning of cellular cholesterol between the PM and interior membrane compartments and/or affect the size of cellular cholesterol pools. To study the potential effect of NPC1 overexpression on cellular distribution of cholesterol, cells were labeled with [^{3}H]cholesterol and treated with cholesterol oxidase, which oxidizes cholesterol to cholestenone. Quantification of [^{3}H]cholestenone (cholesterol in the oxidase-accessible pool) and unesterified [^{3}H]cholesterol provides a measure of PM and intracellular cholesterol pools, respectively (25). We performed these studies under conditions of lipoprotein starvation in the presence and in the absence of compactin, an inhibitor of *de novo* cholesterol synthesis. As compared with wild-type CHO cells, M12 cells grown in the absence of compactin demonstrated a modest reduction (26% decrease) in the cholesterol content of the oxidase-accessible (PM) pool (Fig. 6, *black bars*). This finding is consistent with the defect in M12 cells in mobilization of endosomal cholesterol to the PM. In contrast, NPC1-overexpressing cell lines demonstrated a dose-dependent increase in PM cholesterol content (up to 2.9-fold) in the absence of compactin. Strikingly, growth of CHO/NPC1 cells in the presence of compactin (Fig. 6, *gray bars*) reduced PM cholesterol to levels below that of wild-type CHO cells, whereas intracellular cholesterol levels were increased up to 2.5-fold. As a percentage of the values for wild-type CHO cells, total cellular cholesterol in CHO/NPC1 cells was increased (up to 1.5-fold) and did not significantly differ in the presence or absence of compactin. Taken together, these findings suggest that the increase in PM cholesterol (in the absence of compactin) in the CHO/NPC1 cell lines is due primarily to *de novo* cholesterol synthesis. Moreover, the redistribution of cholesterol from the PM to the cell interior in the setting of inhibition of *de novo* cholesterol synthesis implies a role for NPC1 in internalization of PM cholesterol.

To examine the mechanism of the excess sterol accumulation in the PM of CHO/NPC1 cells, we measured rates of *de novo* cholesterol biosynthesis. CHO, M12, and CHO/NPC1 cell lines were incubated in medium B and pulsed with [^{14}C]acetate, and incorporation of [^{14}C]acetate into [^{14}C]cholesterol was measured. As a control, we also assessed *de novo* synthesis in CT60 cells, which are resistant to sterol suppression because of a D443N SCAP mutation (26, 27) and, therefore, would be expected to show increased cholesterol synthesis relative to wild-type CHO cells. The rate of cholesterol synthesis in the M12 cells did not differ significantly from wild-type CHO cells (Fig. 7). By comparison, the rate of cholesterol synthesis in the NPC1–1 cells was 3-fold greater than that of wild-type CHO cells. For both of the NPC1-overexpressing cell lines studied,

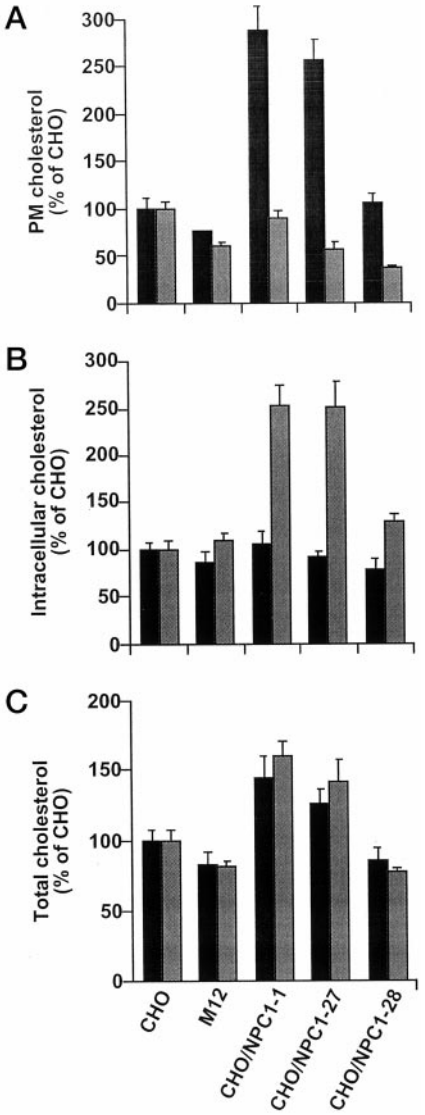

FIG. 6. **Altered distribution of cholesterol in NPC1-overexpressing cell lines.** Cells were plated in triplicate (5×10^4 cells/35-mm well) in medium A for 48 h. The media was replaced with medium B or medium C, and the cells were pulsed with [^{3}H]cholesterol (1 μCi/well). The cells were fixed and treated with cholesterol oxidase and sphingomyelinase, and lipids were extracted and analyzed by TLC. Incorporation of [^{3}H]cholesterol into the PM cholesterol (*A*), intracellular cholesterol (*B*), and total cellular cholesterol (*C*) pools were determined in the absence (*black bars*) and presence of compactin (*gray bars*). Values are means ± S.E. and are representative of two independent experiments.

the rate of *de novo* synthesis (301% of CHO for NPC1–1, 108% of CHO for NPC1–28) closely paralleled the increase in PM cholesterol levels (286% of CHO for NPC1–1, 105% of CHO for NPC1–28).

To determine whether up-regulation of *de novo* cholesterol synthesis was mediated by altered sterol homeostatic mechanisms involving SREBPs, we compared the ability of 25-HC to suppress SRE-dependent gene transcription in CHO and CHO/NPC1 cells. CT60 cells were included as a control, since they are known to be sterol-resistant (26, 27). Cells were transfected with pCMVβgal and the pSyn SRE vector, which contains three SREs from the 3-hydroxy-3-methylglutaryl-coenzyme A synthase gene linked to a luciferase reporter. SRE-containing reporter constructs serve as an indicator of the status of SREBP maturation (13, 18). The luciferase activity in the transfected cells was normalized to β-galactosidase expression to correct

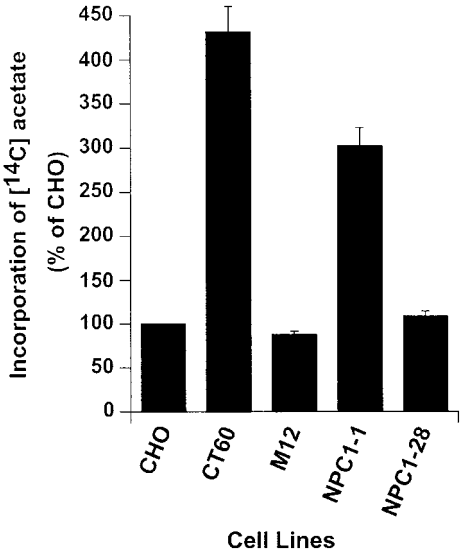

FIG. 7. **CHO/NPC1 cells exhibit increased *de novo* cholesterol synthesis.** On day 0, cells were plated in triplicate (2.5×10^4 cells/35-mm well) in medium A. On day 1, the media was replaced with medium B. On day 2, the cells were refed medium B and pulsed with 0.5 mM [^{14}C]acetate for 2 h. Lipids were extracted and analyzed by TLC, and incorporation of [^{14}C]acetate into [^{14}C]cholesterol was quantified. Values are means ± S.E. and are representative of two independent experiments.

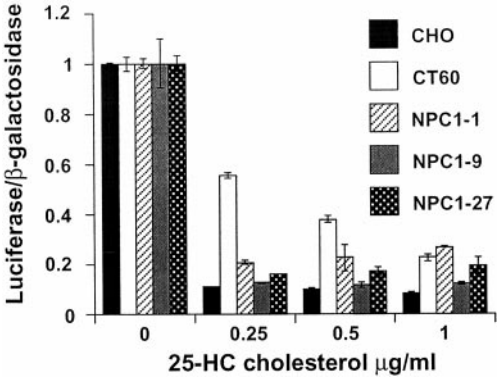

FIG. 8. **NPC1 overexpression inhibits sterol suppression of pSyn SRE expression.** On day 0, CHO, CT60, and CHO/NPC1 cells were plated in duplicate (6×10^5 cells/60-mm dish) in medium A. On day 1, the cells were co-transfected with 1.5 μg of pSyn SRE and 0.5 μg of pCMVβgal. Four hours post-transfection, the media was changed to medium C supplemented with 0–1.0 μg/ml 25-HC. On day 2, cells were harvested, and luciferase and β-galactosidase assays were performed in duplicate. Luciferase activity is normalized for β-galactosidase expression, and data are expressed as mean % activity of 0 μg/ml 25-HC ±S.E. The results are representative of four independent experiments.

for transfection efficiency. As expected, CHO cells responded to incubation with 25-HC by suppression of SRE-dependent transcription at 0.25 μg/ml 25-HC, whereas CT60 cells were resistant to suppression (Fig. 8). CHO/NPC1 cells also failed to suppress to wild-type levels. Resistance to suppression in these cells increased in a dose-dependent manner with increasing oxysterol concentration, whereas resistance in CT60 cells diminished with increasing oxysterol concentration. In four independent experiments, the degree of resistance correlated with the level of NPC1 expression (NPC1–1 > NPC1–9 > NPC1–27). At the highest 25-HC concentration (1 μg/ml), CHO/NPC1 cells were more resistant than CT60 cells.

ER cholesterol levels are thought to play a central role in cholesterol homeostasis through regulation of SCAP/SREBP function (4). To determine whether the perturbations of SCAP/SREBP function in CHO/NPC1 cells resulted from alteration of

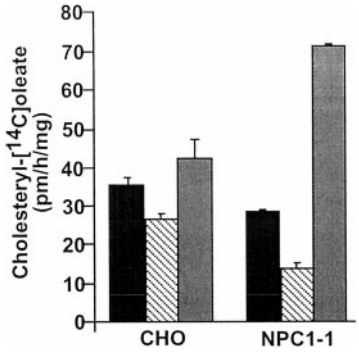

FIG. 9. **Measurement of ER cholesterol pool in CHO/NPC1 cells.** CHO, CHO/NPC1, and CT60 cells were plated in triplicate in medium A and grown to 50% confluence in 6-cm dishes. The cells were then refed either medium B, medium C, or medium C plus 1 μg/ml 25-HC. After 24 h, the cells were homogenized, and the extracts were incubated with [^{14}C]oleoyl-CoA for 1 h at 37 °C. Lipids were extracted, and incorporation of [^{14}C]oleoyl-CoA into [^{14}C]cholesteryl oleate was quantified by TLC. *Black*, *hatched*, and *gray bars* depict measurements made under conditions of lipoprotein starvation, lipoprotein starvation plus compactin, and lipoprotein starvation plus compactin and 25-HC, respectively. Values are means ± S.E. and are representative of three independent experiments.

ER cholesterol pools, we used an *in vitro* cholesterol esterification assay to measure the ER cholesterol content in CHO and CHO/NPC1 cells under various growth conditions. Under conditions of lipoprotein starvation (the conditions under which cholesterol distribution measurements and *de novo* cholesterol synthesis assays were performed), ER cholesterol levels in the CHO/NPC1 cells were reduced 20% as compared with wild-type CHO cells (Fig. 9). The low ER cholesterol content in these cells likely contributes to the increase in *de novo* cholesterol synthesis, which was observed despite increased total cellular cholesterol levels. As expected, under conditions of lipoprotein starvation in the presence of compactin (the conditions under which SRE-dependent gene transcription assays and cholesterol distribution measurements were performed), the ER cholesterol levels in CHO/NPC1 and wild-type CHO cells showed a decline. Previous studies show that treatment with 25-HC promotes marked influx of cholesterol into the ER and propose this as an important mechanism of oxysterol-induced suppression of SCAP-mediated SREBP proteolysis (28). The addition of 25-HC stimulated influx of cholesterol into the ER of the CHO/NPC1 cells (5.1-fold increase), resulting in ER cholesterol levels in the CHO/NPC1 cells (71.2 pm/hr/mg) exceeding that of wild-type CHO cells (42.3 pm/h/mg). Thus, oxysterol-mediated influx of cholesterol into the ER is intact in the CHO/NPC1 cells, suggesting the sterol-resistant phenotype results from another mechanism.

DISCUSSION

In this study we examined the effect of NPC1 overexpression on regulation of cellular cholesterol homeostasis. We generated stable CHO/NPC1 cells and characterized these cell lines by examining the subcellular distribution of NPC1 and by assessment of cholesterol trafficking. We demonstrate by immunofluorescence that the NPC1 protein in the CHO/NPC1 cell lines distributes to appropriate cellular locations. Consistent with previous studies, we show that under normal conditions the NPC1 protein resides in granular cytosolic structures, and after pharmacologic block of cholesterol trafficking, accumulates in a cholesterol-rich endosomal compartment (9). Furthermore, we demonstrate that in a dose-dependent manner, overexpression of NPC1 stimulates intracellular cholesterol trafficking in pathways in which NPC1 is known to participate, including the delivery of LDL-derived cholesterol to acyl-CoA:

cholesterol *O*-acyltransferase and the mobilization of endosomal cholesterol to the PM (2, 3, 10, 11). Based on these findings, we conclude that the sterol-related phenotype of the CHO/NPC1 cells is due to overexpression of functional NPC1 protein.

In the present study several observations indicate that cholesterol homeostasis in NPC1-overexpressing cells is perturbed. First, CHO/NPC1 cells demonstrate a marked increase in PM cholesterol and total cellular cholesterol levels. We show that *de novo* cholesterol synthesis is responsible for the increase in PM cholesterol because inhibition of cholesterol synthesis completely abrogates the increase in PM cholesterol. Moreover, the increased rates of cholesterol synthesis (3-fold) in the CHO/NPC1 cells closely parallel the increase in the PM sterol content (2.9-fold). Second, under conditions of cholesterol starvation, CHO/NPC1 cells exhibit a striking redistribution of cholesterol from the PM to the cell interior. In the absence of *de novo* cholesterol synthesis, PM cholesterol is reduced to levels below that of wild-type CHO cells, even in the cell line with the lowest level of NPC1 expression (NPC1–28). These findings imply an unsuspected role for NPC1 in trafficking of PM cholesterol to intracellular membranes. Third, ER cholesterol levels in the CHO/NPC1 cells are decreased by 20% as compared with wild-type CHO cells. Although the mechanism underlying this decrease is unclear, it is possible that overexpression of NPC1 may adjust the set-point of the ER cholesterol levels either by stimulating cholesterol trafficking or altering the cholesterol content of specific cellular compartments (28). Fourth, despite appropriate oxysterol stimulation of cholesterol movement to the ER, CHO/NPC1 cells fail to effectively suppress SREBP cleavage.

What is the mechanism by which NPC1 overexpression disrupts normal regulation of sterol homeostasis? The increase in cholesterol synthesis in the CHO/NPC1 cells is inappropriate given their increased total cellular cholesterol. Low basal ER cholesterol levels likely provide a stimulus for SREBP proteolysis and thereby contribute to the increased rate of *de novo* cholesterol synthesis. However, appropriate 25-HC-stimulated movement of cholesterol to the ER occurs in CHO/NPC1 cells, and this influx of cholesterol fails to suppress SRE-dependent gene expression. It is possible that the ER cholesterol in CHO/NPC1 cells is unavailable for regulation of SREBP proteolysis. Alternatively, NPC1 may directly interfere with SCAP/SREBP function. In a recent study, overexpression of the sterol-sensing domain (SSD) of SCAP prevented suppression by sterols of SCAP/SREBP movement to the Golgi (24). A model has been proposed in which the SCAP/SREBP complex binds to an ER retention protein through an interaction involving the SSD of SCAP. The overexpressed SCAP SSD competes with the SCAP/SREBP complex for binding to the putative retention protein, allowing the complex to move to the Golgi despite the presence of sterols. Similarly, overexpression of the SSD-containing NPC1 may interfere with sterol regulation of SCAP/SREBP movement by competing with SCAP for binding to this putative retention protein. Elucidation of the molecular function of NPC1, in general, and of the SSD, in particular, will shed light on the role of this protein in sterol homeostasis.

Acknowledgments—We thank Peter Pentchev for helpful discussions and the Ara Parseghian Medical Research Foundation for providing a forum for scientific discussions.

REFERENCES

1. Brown, M. S., and Goldstein, J. L. (1983) *Annu. Rev. Biochem.* **52,** 223–261
2. Neufeld, E. B., Cooney, A. M., Pitha, J., Dawidowicz, E. A., Dwyer, N. K., Pentchev, P. G., and Blanchette-Mackie, E. J. (1996) *J. Biol. Chem.* **271,** 21604–21613
3. Underwood, K. W., Jacobs, N. L., Howley, A., and Liscum, L. (1998) *J. Biol. Chem.* **273,** 4266–4274
4. Brown, M. S., and Goldstein, J. L. (1997) *Cell* **89,** 331–340
5. Liscum, L., and Faust, J. R. (1987) *J. Biol. Chem.* **262,** 17002–17008
6. Carstea, E. D., Morris, J. A., Coleman, K. G., *et al.* (1997) *Science* **277,** 228–231
7. Loftus, S. K., Morris, J. A., Carstea, E. D., Gu, J. Z., Cummings, C., Brown, A., Ellison, J., Ohno, K., Rosenfeld, M. A., Tagle, D. A., Pentchev, P. G., and Pavan, W. J. (1997) *Science* **277,** 232–235
8. Davies, J. P., and Ioannou, Y. A. (2000) *J. Biol. Chem.* **275,** 24367–24374
9. Neufeld, E. B., Wastney, M., Patel, S., Suresh, S., Cooney, A. M., Dwyer, N. K., Roff, C. F., Ohmo, K., Morris, J. A., Carstea, E. D., Incardoma, J. P., Strauss, J. F., III, Vanier, M. T., Patterson, M. C., Brady, R. O., Pentchev, P. G., and Blanchette-Mackie, E. J. (1999) *J. Biol. Chem.* **274,** 9627–9635
10. Liscum, L., and Faust, J. R. (1989) *J. Biol. Chem.* **264,** 11796–11806
11. Cruz, J. C., Sugii, S., Yu, C., and Chang, T. Y. (2000) *J. Biol. Chem.* **275,** 4013–4021
12. Ory, D. S., Neugeboren, B. A., and Mulligan, R. C. (1996) *Proc. Natl. Acad. Sci. U. S. A.* **93,** 11400–11406
13. Worgall, T. S., Sturley, S. L., Seo, T., Osborne, T. F., and Deckelbaum, R. J. (1998) *J. Biol. Chem.* **273,** 25537–25540
14. Brown, M. S., Dana, S. E., and Goldstein, J. L. (1973) *Proc. Natl. Acad. Sci. U. S. A.* **70,** 2162–2166
15. Krieger, M., Brown, M. S., Faust, J. R., and Goldstein, J. L. (1978) *J. Biol. Chem.* **253,** 4093–4101
16. Stuhlsatz-Krouper, S. M., Bennett, N. E., and Schaffer, J. E. (1998) *J. Biol. Chem.* **273,** 28642–28650
17. Goldstein, J. L., Basu, S. K., and Brown, M. S. (1983) *Methods Enzymol.* **98,** 241–260
18. Rawson, R., Cheng, D., Brown, M. S., and Goldstein, J. L. (1998) *J. Biol. Chem.* **273,** 28261–28269
19. Lange, Y., and Steck, T. L. (1997) *J. Biol. Chem.* **272,** 13103–13108
20. Patel, S. C., Suresh, S., Kumar, U., Hu, C. Y., Cooney, A., Blanchette-Mackie, E. J., Neufeld, E. B., Patel, R. C., Brady, R. O., Patel, Y. C., Pentchev, P. G., and Ong, W. I. (1999) *Proc. Natl. Acad. Sci. U. S. A.* **96,** 1657–1662
21. Watari, H., Blanchette-Mackie, E. J., Dwyer, N. K., Glick, J. M., Patel, S., Neufeld, E. B., Brady, R. O., Pentchev, P. G., and Strauss, J. F., III (1999) *Proc. Natl. Acad. Sci. U. S. A.* **96,** 805–810
22. Pentchev, P. G., Comly, M. E., Kruth, H. S., Vanier, M. T., Wenger, D. A., Patel, S., and Brady, R. O. (1985) *Proc. Natl. Acad. Sci. U. S. A.* **82,** 8247–8251
23. Barasch, J., Kiss, B., Prince, A., Saiman, L., Gruenert, D., and Al-Awqti, Q. (1991) *Nature* **352,** 70–73
24. Yang, T., Goldstein, J. L., and Brown, M. S. (2000) *J. Biol. Chem.* **275,** 29881–29886
25. Slotte, J. P., Hedstrom, G., Rannstrom, S., and Ekman, S. (1989) *Biochim. Biophys. Acta* **985,** 90–96
26. Cadigan, K. M., Spillane, D. M., and Chang, T. Y. (1990) *J. Cell Biol.* **110,** 295–308
27. Hua, X., Nohturfft, Goldstein, J. L., and Brown, M. S. (1996) *Cell* **87,** 415–426
28. Lange, Y., Ye, J., Rigney, M., and Steck, T. L. (1999) *J. Lipid Res.* **40,** 2264–2270